



Search for W' Boson Production in the Single Top Quark Channel at DØ in Run II

The DØ Collaboration
<http://www-d0.fnal.gov>
(Dated: March 8, 2006)

We present a search for production of a new heavy gauge boson W' that decays to a top quark and a bottom quark. We have analyzed 230 pb^{-1} of data collected with the DØ detector at the Fermilab Tevatron collider at a center-of-mass energy of $\sqrt{s} = 1.96 \text{ TeV}$. No significant excess of events is found in any region of the final state invariant mass distribution. We set upper limits on the production cross section of W' bosons at the 95% confidence level. For a W' boson mass of 600 GeV (700 GeV, 800 GeV) the upper limit is 1.8 pb (1.4 pb, 2.2 pb). We exclude the mass range between 200 GeV and 650 GeV for a W' boson with Standard Model-like couplings.

Preliminary Results for Winter 2006 Conferences

I. INTRODUCTION

The top quark sector offers great potential to look for new physics related to electroweak symmetry breaking. In particular, it is a sensitive probe to the presence of additional gauge bosons beyond the W boson of the Standard Model (SM). Such additional gauge bosons W' and Z' typically arise in extensions to the SM from the presence of additional symmetry groups [1, 2].

The top quark was discovered in 1995 by the CDF and DØ collaborations [3], but SM single top quark production has not yet been observed. Both collaborations have performed searches for single top quark production in Run II [4, 5]. At the 95% confidence level, the limit measured by DØ on the s -channel process is 5 pb, and the limit measured by CDF is 13.6 pb. At the same confidence level, the limit on the t -channel production cross section is 4.4 pb from DØ and 10.1 pb from CDF.

Direct searches for the production of additional heavy gauge bosons W' have focused on the lepton final state which has good separation between the W' boson signal and the SM backgrounds. The W' boson lower mass limit in this decay channel is 786 GeV [7]. However, it is also possible that such a W' boson does not interact with leptons and neutrinos but only with quarks. Previous direct searches for the presence of W' bosons in the quark decay channel have excluded the mass range below 261 GeV [8] and between 300 GeV and 420 GeV [9]. Assuming that the W' boson decays only to quarks and not to leptons yields a lower mass limit of 800 GeV [10]. Indirect searches for evidence of a W' boson depend on exactly how it interferes with the SM W boson and the results are thus highly model specific (see Ref. [2] and references therein).

The single top quark final state is especially sensitive to the presence of an extra heavy boson, owing to the decay chain $W' \rightarrow t\bar{b}$, where the top quark decays to a b quark and a SM W boson. This decay is kinematically allowed as long as the W' mass is larger than the sum of top and bottom quark masses, i.e. as long as it is above about 200 GeV.

An extra heavy boson would appear as a peak in the invariant mass distribution of the $t\bar{b}$ final state. The leading order Feynman diagram for W' boson production resulting in single top quark events is shown in Fig. 1. This diagram is identical to that for s -channel SM single top quark production where the SM W boson appears as the virtual particle [11–14].

The W' boson also has a t -channel exchange that leads to a single top quark final state. However, the cross section for a t -channel W' process is much smaller than the SM t -channel single top quark production due to the high mass of the W' boson. It will thus not be considered in this note.

The top quark then decays to a b quark and a SM W boson, which in turn decays leptonically or hadronically. The heavy W' boson also could contribute to this decay, but that contribution is negligible, again because of the large mass of the W' boson, and will not be considered here.

In this note, we make the assumption that the coupling of the W' boson to the SM fermions is identical to that of the SM W boson. We further assume that the CKM mixing matrix element for the W' boson is one. Under these assumptions, there is interference between the SM s -channel process and the W' boson production process from Fig. 1. This is different from Refs. [9, 10] which did not take interference terms into account.

This interference term is small for large W' boson masses, but it becomes important in the invariant mass range of a few hundred GeV where the SM s -channel production cross section is large. In our modeling of the W' boson production process, we take the interference with the SM W boson process into account. Table I shows the NLO

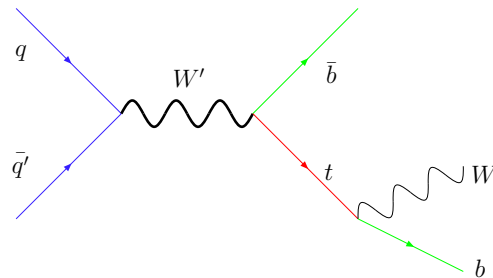


FIG. 1: Leading order Feynman diagram for single top quark production via a heavy W' boson. The top quark decays via a SM W boson.

cross sections for single top quark production through a W' boson with SM-like couplings. The cross section takes into account the Feynman diagram from Fig. 1 as well as the SM s -channel diagram and the interference between the two. This combined cross section has been calculated at leading order with CompHEP [18], and then scaled to NLO with a k -factor based on Ref. [2], Table VII.

This analysis focuses on the final state topology of single top quark production where the top quark decays into a b quark and a SM W boson, which subsequently decays leptonically ($W \rightarrow e\nu, \mu\nu$). This is the first analysis to

TABLE I: Production cross section for a W' boson with SM like couplings times decay branching ratio to a top and a bottom quark, computed at leading order and scaled to NLO according to Ref. [2]. The W' boson production cross sections include the SM s -channel contribution as well as the interference term between the two. The uncertainty includes contributions due to renormalization and factorization scale, PDFs, and top quark mass.

Cross section \times BR($W' \rightarrow t\bar{b}$) [pb]	
W' (600 GeV)	2.17 ($\pm 12\%$)
W' (700 GeV)	1.03 ($\pm 13\%$)
W' (800 GeV)	0.65 ($\pm 18\%$)

investigate this particular final state of W' boson decays. It gives rise to an event signature with a high transverse momentum lepton and significant missing transverse energy from the neutrino, in association with two b quark jets. The largest backgrounds to this event signature come from W +jets and $t\bar{t}$ production. We also consider SM t -channel single top quark production as a background in this search.

The theoretical W' boson production cross section is more than 15 pb for masses between 200 GeV and 400 GeV [2]. The current limits on single top quark production are below this value and thus rule out a W' boson in this mass region. The current limit on the s -channel production cross section is 6.4 pb from a neural network analysis [5] and 13.0 pb from simple event counting [6]. In this analysis we explore the region of even higher mass W' boson production.

The analysis proceeds as follows. We use the same dataset, basic event selection, and background modeling as the first Run II single top quark search publication [5]. We select signal-like events and separate the data into independent analysis sets based on final state lepton flavor (electron or muon) and b -tag multiplicity (single tagged and double tagged), where b quark jets are tagged using reconstructed displaced vertices in the jets. The independent analysis sets are later combined in the final statistical analysis. We perform a binned likelihood analysis on the invariant mass distribution of all final state objects to obtain cross section limits at discrete W' mass points. We then compare these limits at each mass point to the theoretical prediction and derive a limit on the mass of the W' boson.

II. THE DØ DETECTOR

The DØ detector in Run II consists of a central tracking system, a liquid-argon/uranium calorimeter, and an iron toroid muon spectrometer [16]. The central tracking system includes a silicon microstrip tracker and a central fiber tracker, both located within a 2 T superconducting solenoidal magnet. The calorimeters consist of a central module covering the detector pseudorapidity region $|\eta_{\text{det}}| < 1.1$ and two end calorimeters extending the coverage to $|\eta_{\text{det}}| < 4.2$ [17]. The muon system resides outside the calorimeter, and consists of a layer of tracking detectors and scintillation counters before 1.8 T toroids, followed by two similar layers after the toroids. Luminosity is measured using plastic scintillator arrays located in front of the end calorimeters.

III. DATA AND EVENT SELECTION

The analysis is based on electron and muon events recorded between August 2002 and March 2004. The data were collected using a trigger that required an electromagnetic energy cluster and a jet in the calorimeter for the electron channel, and a muon and a jet for the muon channel. The integrated luminosity is $230 \pm 15 \text{ pb}^{-1}$ for both lepton channels. The event selection is identical to that in Ref. [5], except that only events with two or three jets are allowed, four-jet events are excluded to reduce the background contribution from $t\bar{t}$ production.

In the electron channel, candidate events are selected by requiring exactly one isolated electron (based on a seven-variable likelihood) with $E_T > 15 \text{ GeV}$ and $|\eta_{\text{det}}| < 1.1$. In the muon channel, events are selected by requiring exactly one isolated muon with $p_T > 15 \text{ GeV}$ and $|\eta_{\text{det}}| < 2.0$. For both channels, the events are also required to have missing transverse energy $\cancel{E}_T > 15 \text{ GeV}$. Jets are required to have $E_T > 15 \text{ GeV}$ and $|\eta_{\text{det}}| < 3.4$. Events must have exactly two or exactly three jets, with the leading jet additionally required to have $E_T > 25 \text{ GeV}$ and $|\eta_{\text{det}}| < 2.5$. Misreconstructed events are rejected by requiring that low \cancel{E}_T is not aligned or anti-aligned with leptons or jets. We require at least one b -tagged jet and separate the dataset into orthogonal sets based on whether one or two jets are b -tagged.

Secondary-vertex tagging is used to identify displaced vertices of long-lived particles like those from B hadrons. To form secondary vertices, charged tracks are selected on the basis of the significance of their distance of closest approach (d_{ca}) to the primary vertex. Tracks are first grouped in cones of radius $R = \sqrt{(\Delta\eta)^2 + (\Delta\phi)^2} = 0.5$ around a seed

track with $p_T > 1$ GeV and $d_{ca}/\sigma_{d_{ca}} > 3.5$, where $\sigma_{d_{ca}}$ is the uncertainty on the d_{ca} of the track. Secondary vertices are selected by requiring the decay-length significance $L_{xy}/\sigma_{L_{xy}}$ to be greater than 7, where L_{xy} is the decay-length and $\sigma_{L_{xy}}$ is the estimated uncertainty on L_{xy} , calculated from the error matrices of the tracks and the primary vertex. Jets are considered tagged by this algorithm when a secondary vertex lies within a cone of $R = 0.5$ of the original jet axis.

IV. SIGNAL AND BACKGROUND MODELING

We estimate the acceptances for W' boson production of single top quarks using events generated by the COMPHEP matrix element event generator [18]. The same program is used to estimate the yield for the SM single top quark background. Interference between the SM s -channel and W' production is taken into account in the COMPHEP event generation, and the label W' in the event yield tables below includes both SM s -channel and W' boson production. The W' boson signals are normalized to the NLO cross section from Table I, and we use the CTEQ6L1 parton distribution functions [19].

We use both Monte Carlo and data to estimate the other background yields. The W +jets and diboson (WW and WZ) backgrounds are estimated using Monte Carlo events generated with ALPGEN [20]. The diboson background yield is normalized to NLO cross sections computed with MCFM [21]. The overall W +jets yield is normalized to the data sample before requiring a b -tagged jet, and the fraction of heavy-flavor ($Wb\bar{b}$) events is found using MCFM with the same parton-level cuts applied as for the samples used in the simulation. This normalization to data also accounts for smaller contributions such as Z +jets events, where one of the leptons from the Z boson decay is not reconstructed. The $t\bar{t}$ background is estimated using Monte Carlo samples generated with ALPGEN, normalized to the (N)NLO cross section calculation: $\sigma(t\bar{t}) = 6.7 \pm 1.2$ pb [22]. The SM t -channel background is normalized to the NLO cross section calculation: $\sigma(tqb) = 1.98 \pm 0.32$ pb [11]. In both cases, the uncertainty on the top quark mass is taken into account in the cross section uncertainty. The parton-level samples are then processed with PYTHIA [23] and a GEANT [24]-based simulation of the DØ detector, and the resulting lepton and jet energies are smeared to reproduce the resolutions observed in data. Both the shape and the overall normalization of the multijet background is estimated from data, using multijet data samples that pass all event selection cuts but fail the electron likelihood requirement in the electron channel or the muon isolation requirement in the muon channel.

Estimates for signal and background yields as well as the observed number of events after selection are shown in Table II.

TABLE II: Event yields after selection, for the electron and muon channel, single b -tags and double b -tags combined. The W +jets row includes Wjj , Wbb , WW , and WZ .

<u>Event Yields after Selection</u>	
Signals	
W' (600 GeV)	25.2
W' (700 GeV)	11.5
W' (800 GeV)	7.0
Backgrounds	
SM t -channel	7.7
$t\bar{t}$	44.8
W +jets	160.8
Multijet	27.0
Background sum	240.3
Data	232

V. FINAL ANALYSIS

The large mass of the W' boson sets it apart from all background processes, hence the best place to look for such a particle is to reconstruct its invariant mass in the resonance production process. We reconstruct the invariant mass of the W' boson (the invariant mass of all final state objects) by adding the four-vectors of all reconstructed final state objects: the quark jets, the lepton, and the neutrino from the W boson decay from the top quark decay. The

xy -components of the neutrino momentum are given by the missing transverse energy. The z -component is calculated using a SM W boson mass constraint, choosing the solution with smaller $|p_z^{\nu}|$ from the two possible solutions.

Figure 2 shows the reconstructed W' boson invariant mass distribution for three representative W' boson masses and representative background contributions. The background contributions all peak at invariant masses below 400 GeV,

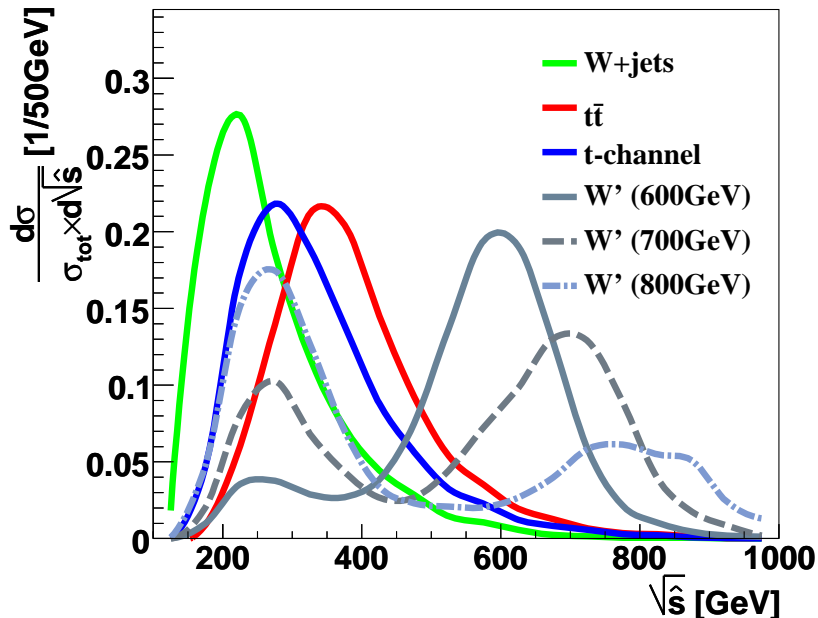


FIG. 2: Distribution of the reconstructed W' boson invariant mass normalized to unit area for several different W' boson masses as well as background processes.

and extend out to about 800 GeV. Since the signal distributions include contributions from a W' boson and the SM s -channel, they show two peaks. One is at the invariant mass of the W' boson, and the other one is at the lower end where SM s -channel production dominates. The relative height of the two peaks give some idea of the relative weight of the two contributions. For a W' boson mass of 600 GeV, the W' contribution is significantly larger than the SM s -channel contribution, while for a W' boson mass of 800 GeV, the SM s -channel contribution is larger.

Figure 3 shows a comparison of the invariant mass distribution in data to the sum of all background processes. Also shown are the expected contributions for three different W' boson mass points.

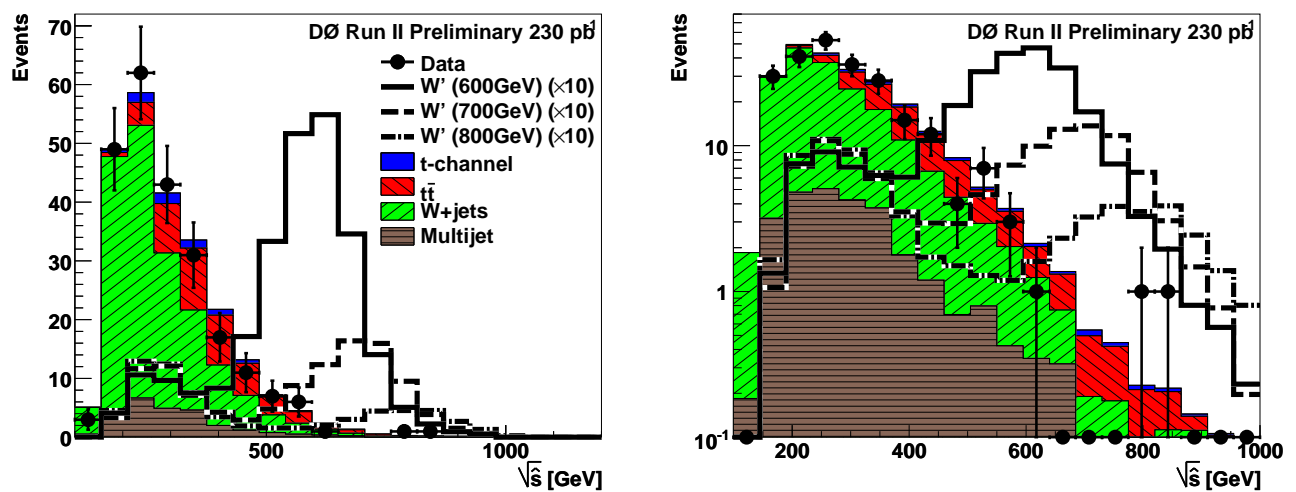


FIG. 3: Reconstructed W' boson invariant mass for several different W' boson masses as well as background processes. Electron, muon, single b -tagged, and double b -tagged events are included. The left histogram has a linear vertical scale, the right histogram a log vertical scale.

There are two events at an invariant mass of more than 800 GeV, with an expected background of about 0.5 events. Though this is an excess of events, it is within uncertainties and consistent with an upward fluctuation of the background. Moreover, both events appear in the single-tagged muon channel, and it appears that in one of them, the muon momentum has been mismeasured. Thus the observation, overall, is consistent with the background model.

VI. SYSTEMATIC UNCERTAINTIES

Systematic uncertainties are evaluated for the Monte Carlo signal and background samples, separately for electrons and muons and for each b -tag multiplicity. The dominant sources of systematic uncertainty on the signal and background acceptances are (a) the uncertainty on the b -tag modeling in the Monte Carlo, (b) the uncertainty from the jet energy scale, (c) 5% uncertainty on the object identification efficiencies, (d) 5% uncertainty on the trigger modeling, and (e) 5% uncertainty on the modeling of jet fragmentation. Each of these systematic uncertainties has been evaluated by varying the uncertainty for each object in the event (electrons, muons, jets) up and down by one standard deviation, and then propagating the updated objects and corresponding weights through the analysis chain. The uncertainty on the integrated luminosity is 6.5% [25]. The background yields also have uncertainties from the cross section, which vary from 8% for diboson production to 15% for SM t -channel single top quark production and 18% for the $t\bar{t}$ samples [22]. Since the W +jets background is normalized to the data before tagging, the yield estimate is only affected by uncertainties related to b -tagging. These include the b -tag modeling uncertainty, and the uncertainty in the flavor composition before tagging, which is estimated at 25%.

For the different background contributions, the jet energy scale uncertainty varies between 15% and 30%. This uncertainty is large in the background samples because most events have a small invariant mass and only very few events are in the region $\sqrt{\hat{s}} > 400$ GeV. Changing the jet energy by a small amount doesn't change the overall distribution very much but it has a large impact on the number of events in the region $\sqrt{\hat{s}} > 400$ GeV. The uncertainty from b -tag modeling is about 8% in the single b -tagged sample and about 20% in the double b -tagged sample. The total uncertainty on the multijet samples is very large due to the small number of events in the data sample used to model this background.

Due to their similar kinematic properties, the three W' boson signal processes all have very similar systematic uncertainties. The jet energy scale systematic uncertainty is small (1%-2%) for the signal processes because most of the signal events are in the region $\sqrt{\hat{s}} > 400$ GeV. The uncertainty for the signal samples has significant contributions from b -tag modeling (4% for the single b -tagged, 16% for the double b -tagged sample) and trigger modeling.

Table III shows the event yield in the region $\sqrt{\hat{s}} > 400$ GeV used for the binned likelihood analysis for all samples, including the total systematic uncertainty. The yield for the W' samples has been calculated from the cross sections given in Table I, and the yield uncertainty includes both the acceptance uncertainty and the cross section uncertainty.

The acceptance for signal events with at least one b -tagged jet and requiring $\sqrt{\hat{s}} > 400$ GeV is $4.0 \pm 0.4\%$ ($5.1 \pm 0.5\%$, $1.2 \pm 0.1\%$) for a W' boson mass of 600 GeV (700 GeV, 800 GeV). The acceptance for the exclusive W' boson part is fairly large, while the acceptance for the exclusive SM s -channel part is much smaller (1%) due to the differences in event kinematics. The total acceptance is a combination of the two and depends on the relative cross sections and the interference term, which changes with W' boson mass, see Fig. 2. The uncertainty includes all contributions listed above, but not the cross section uncertainty.

VII. CROSS SECTION LIMITS

The observed data are consistent with the background predictions within uncertainties. We therefore set upper limits on the W' boson production cross section for different W' boson masses using a Bayesian approach [26]. We follow the formalism given in Ref. [5]. The limits are derived from a likelihood function that is proportional to the probability to obtain the number of observed counts. We form binned likelihoods based on the final state invariant mass distribution. We assume a Poisson distribution for the observed counts, and a flat prior probability for the signal cross section. The priors for the signal acceptance and the background yields are multivariate Gaussians centered on their estimates and described by a covariance uncertainty matrix taking into account correlations across the different sources and bins. We assign source-dependent systematic uncertainties but no bin-dependent systematic uncertainty. As a measure of the sensitivity of the analysis we also compute expected cross section limits for each W' boson mass. These correspond to the limits calculated when the observed count in each bin is set to the background sum.

We combine the single-tagged and double-tagged analysis channels, as well as the electron and muon channels. Table IV shows the expected and measured cross section limits for two different W' boson masses.

These limits on the production cross section can be compared to the theoretical prediction for the W' production cross section from Table I. Figure 4 shows the limits from Table IV together with the cross sections from Table I. The individual limit points are connected by straight lines. The contribution from a W' boson with SM-like couplings is also shown, and the dashed line is a straight line connecting two neighboring points. Other methods of connecting

TABLE III: Event yields with uncertainty after selection, for the electron and muon channel, single-tagged and double-tagged samples combined, requiring $\sqrt{\hat{s}} > 400$ GeV. The W +jets row includes Wjj , Wbb , WW , and WZ .

Event Yields for $\sqrt{\hat{s}} > 400$ GeV	
Signals	
W' (600 GeV)	21.9 (± 4.2)
W' (700 GeV)	7.9 (± 1.6)
W' (800 GeV)	3.4 (± 0.8)
Backgrounds	
SM t -channel	1.9 (± 0.8)
$t\bar{t}$	16.9 (± 5.6)
W +jets	17.8 (± 4.5)
Multijet	4.4 (± 1.5)
Background sum	40.7 (± 10.2)
Data	30

TABLE IV: Expected and measured 95% confidence level upper limits in picobarns on the production cross section of W' bosons with SM-like couplings. The limits are calculated from a binned likelihood based on the final state invariant mass distribution, for the electron and muon, single- and double-tagged channels combined.

95% CL Expected and measured upper Limits on the W' boson cross section [pb]			
	W' (600 GeV)	W' (700 GeV)	W' (800 GeV)
Statistical uncertainty only			
Expected limit	1.6	1.6	2.1
Measured limit	1.3	1.2	1.9
All uncertainties			
Expected limit	1.8	1.6	2.1
Measured limit	1.7	1.4	2.1

the points would also be possible, for example fitting a higher-order polynomial to the limit points and an exponential to the cross section points. Those approaches would result in roughly the same or slightly higher limits in the W' boson mass, and we use straight lines here for simplicity.

At the 95% C.L., the shaded area above the solid line is excluded by this analysis. The intersection of the solid line with the dashed line defines the lower mass limit for a W' boson with SM-like couplings. The resulting mass limit is 650 GeV.

VIII. SUMMARY

No evidence is found for the presence of a heavy W' boson decaying to a top and a bottom quark in 230 pb $^{-1}$ of data collected with the DØ detector at $\sqrt{s} = 1.96$ TeV. A secondary-vertex reconstruction algorithm has been employed to select events with exactly one or more than one b jet in electron+jets and muon+jets final states. A binned likelihood analysis is performed using the distribution of final state invariant mass. We set limits at the 95% C.L. of 1.8 pb (1.4 pb, 2.1 pb) on the production cross section of a W' boson with a mass of 600 GeV (700 GeV, 800 GeV). Based on these cross section limits, we set a lower limit on the mass of a W' boson of 650 GeV for a W' boson that has SM-like couplings to leptons and quarks. Together with the limit from the SM single top searches we thus exclude W' boson production for masses between 200 GeV and 650 GeV. This is the first limit on W' boson production from single top quark production. While the limits for a W' boson coupling to quarks only are more stringent [10], this analysis extends the exclusion region for W' boson production with SM-like couplings in the quark decay channel by more than 200 GeV [9].

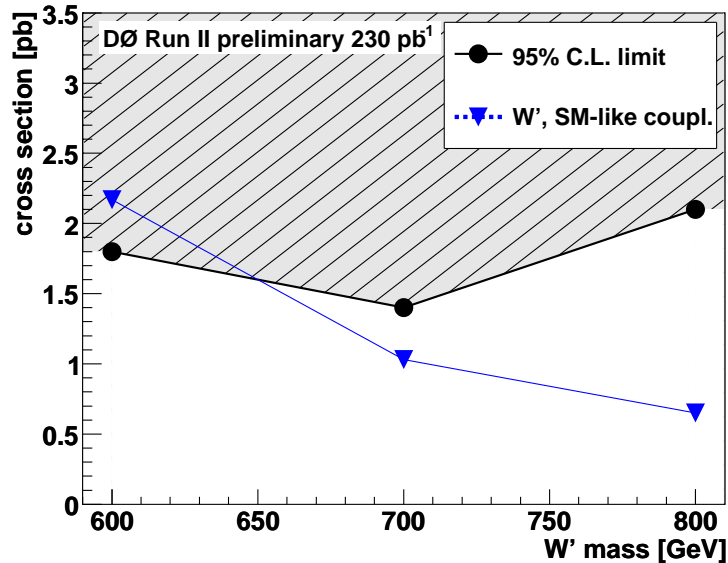


FIG. 4: Cross section limits at the 95% C.L. versus mass of the W' boson. Also shown are the NLO cross sections for a W' boson with SM-like couplings. The shaded region is excluded by this measurement.

Acknowledgments

We are grateful to Tim Tait for discussions that have led us to this search.

We thank the staffs at Fermilab and collaborating institutions, and acknowledge support from the Department of Energy and National Science Foundation (USA), Commissariat à l'Énergie Atomique and CNRS/Institut National de Physique Nucléaire et de Physique des Particules (France), Ministry of Education and Science, Agency for Atomic Energy and RF President Grants Program (Russia), CAPES, CNPq, FAPERJ, FAPESP and FUNDUNESP (Brazil), Departments of Atomic Energy and Science and Technology (India), Colciencias (Colombia), CONACyT (Mexico), KRF (Korea), CONICET and UBACyT (Argentina), The Foundation for Fundamental Research on Matter (The Netherlands), PPARC (United Kingdom), Ministry of Education (Czech Republic), Canada Research Chairs Program, CFI, Natural Sciences and Engineering Research Council and WestGrid Project (Canada), BMBF and DFG (Germany), Science Foundation Ireland, A.P. Sloan Foundation, Research Corporation, Texas Advanced Research Program, and the Alexander von Humboldt Foundation.

-
- [1] T. Tait and C. P. Yuan, *Phys. Rev. D* **63**, 014018 (2001).
 - [2] Z. Sullivan, *Phys. Rev. D* **66**, 075011 (2002).
 - [3] F. Abe *et al.*, [CDF Collaboration], *Phys. Rev. Lett.* **74**, 2626 (1995); S. Abachi *et al.*, [DØ Collaboration], *Phys. Rev. Lett.* **74**, 2632 (1995).
 - [4] D. Acosta *et al.*, [CDF Collaboration], *Phys. Rev. D* **71**, 012005 (2005).
 - [5] V. M. Abazov *et al.* [DØ Collaboration], *Phys. Lett. B* **622**, 265 (2005).
 - [6] V. M. Abazov *et al.* (DØ Collaboration), “Multivariate searches for single top quark production with the DØ detector”, to be submitted to *Phys. Rev. D* (2006).
 - [7] T. Affolder *et al.* [CDF Collaboration], *Phys. Rev. Lett.* **87**, 231803 (2001).
 - [8] J. Alitti *et al.* [UA2 Collaboration], *Nucl. Phys. B* **400**, 3 (1993).
 - [9] F. Abe *et al.* [CDF Collaboration], *Phys. Rev. D* **55**, 5263 (1997).
 - [10] V. M. Abazov *et al.* [DØ Collaboration], *Phys. Rev. D* **69**, 111101 (2004) [arXiv:hep-ex/0308033].
 - [11] B.W. Harris, E. Laenen, L. Phaf, Z. Sullivan, and S. Weinzierl, *Phys. Rev. D* **66**, 054024 (2002).
 - [12] Z. Sullivan, *Phys. Rev. D* **70**, 114012 (2004).
 - [13] J. Campbell, R. K. Ellis and F. Tramontano, *Phys. Rev. D* **70**, 094012 (2004).
 - [14] Q. H. Cao, R. Schwienhorst and C. P. Yuan, *Phys. Rev. D* **71**, 054023 (2005).
 - [15] Q. H. Cao, R. Schwienhorst, J. A. Benitez, R. Brock and C. P. Yuan, *Phys. Rev. D* **72**, 094027 (2005).
 - [16] V. M. Abazov *et al.* [DØ Collaboration], submitted to *Nucl. Instrum. Methods in Phys. Res. A* arXiv:physics/0507191 (2005).

- [17] Pseudorapidity is defined as $\eta = -\ln(\tan \frac{\theta}{2})$, where θ is the polar angle with the origin at the primary vertex. Detector fiducial regions are defined by detector pseudorapidity η_{det} which is calculated with the origin at the nominal center of the detector ($z = 0$).
- [18] E. Boos *et al.*, [CompHEP Collaboration], “CompHEP 4.4: Automatic Computations from Lagrangians to Events,” Nucl. Instrum. Meth. A **534**, 250 (2004);
E.E. Boos, L.V. Dudko, and V.I. Savrin, “SingleTop’ — an Event Generator for the Single Top Quark Production at the LHC,” CMSNote 2000/065.
- [19] J. Pumplin, D. R. Stump, J. Huston, H. L. Lai, P. Nadolsky and W. K. Tung, JHEP **0207**, 012 (2002) [arXiv:hep-ph/0201195].
- [20] M.L. Mangano, M. Moretti, F. Piccinini, R. Pittau, and A.D. Polosa, J. High Energy Physics **0307**, 001 (2003).
- [21] J. Campbell and K. Ellis, “MCFM Monte Carlo for FeMtobarn Processes”; <http://mcfm.fnal.gov>; J. Campbell and K. Ellis, “Next-to-Leading Order Corrections to $W+2$ Jet and $Z+2$ Jet Production at Hadron Colliders,” hep-ph/0202176.
- [22] N. Kidonakis and R. Vogt, Phys. Rev. D **68**, 114014 (2003).
- [23] T. Sjöstrand *et al.*, “PYTHIA 6.2: Physics and Manual,” hep-ph/0108264.
- [24] R. Brun *et al.*, “GEANT - Detector Description and Simulation,” CERN Program Library Long Writeup W 5013 (1994).
- [25] T. Edwards *et al.* [DØ Collaboration], “Determination of the Effective Inelastic $p\bar{p}$ Cross-Section for the DØ Run II Luminosity Measurement,” FERMILAB-TM-2278-E (2004).
- [26] I. Bertram *et al.*, “A Recipe for the Construction of Confidence Limits,” FERMILAB-TM-2104 (2000).